AIAA JOURNAL
Vol. 51, No. 3, March 2013

Broadband Shock-Associated Noise in Screeching and Non-Screeching Underexpanded Supersonic Jets

Benoît André,* Thomas Castelain,† and Christophe Bailly‡
École Centrale de Lyon, 69134 Ecully Cedex, France

DOI: 10.2514/1.J052058

The effect of screech tones on the broadband shock-associated noise of underexpanded jets is investigated experimentally. Screech is removed by means of a notched nozzle, and the properties of the broadband shock-associated noise in the screech-free configuration are compared to that in a screeching flow. It is first demonstrated that the suppressing technique used is nonintrusive in that it does not alter the shock-cell structure of the jet plume. It is then shown that screech has an effect on the aerodynamics of the jet, which induces changes in the broadband shock-associated noise. Indeed, screech accelerates the damping of the shock-cell pattern, leading to an attenuation of the broadband shock-associated noise and a shifting of this noise component to higher frequencies. Moreover, a tuning between the peak frequency of the broadband shock-associated noise and the screech frequency is observed. It is also deduced from the directivity of the broadband shock-associated noise in the far field that the convective velocity in the shear layer is modified in the presence of screech tones.

I. Introduction

A LARGE part of the current commercial aircraft is powered by a high-bypass-ratio engine, in which a hot primary stream is embedded in a cold secondary (fan) flow. At the typical subsonic cruise speeds, the secondary jet becomes imperfectly expanded in flight, which induces a shock-cell structure inside the flow. The interaction of the turbulence in the jet mixing layer with the shock-cell system is responsible for the so-called shock-associated noise component of jet noise, which is in addition to the ever-present turbulent mixing noise. Shock-associated noise is made up of two distinct components: a tonal one, referred to as screech, and a broadband one.

Screech has been extensively studied since Powell's pioneering work [1]. Powell explained with some success the generation of this tone by an acoustic feedback loop between the nozzle and an array of acoustic sources coincident with the shocks. In this model, vorticity disturbances originating from the nozzle lip are convected downstream and interact with the shock-cell pattern of the jet plume. The acoustic waves emanating from this interaction propagate back to the nozzle where they trigger new disturbances, thus closing the loop. This loop is resonant for some frequencies, which are the fundamental screech frequency and its harmonics. The screeching process shows a modal behavior, first identified by Powell and subsequently studied by Merle [2], Davies and Oldfield [3,4], and Powell et al. [5], among others. A summary of the knowledge on screech is provided in Raman [6].

Broadband shock-associated noise (BBSAN) is linked with screech [7] because their generation process is basically the same, apart from the resonant loop. The BBSAN has been studied since Martlew [8]. Harper-Bourne and Fisher [9] adapted Powell's model involving an array of stationary sources to derive some observed properties of this noise component. Tanna [10] performed extensive acoustic measurements to evaluate this semi-analytical model. Much progress on the BBSAN was made around 1980 at NASA by Norum and Seiner [11], who associated advanced aerodynamical measurements, such as static pressure [12] or turbulence fluctuation levels [13], to near-field and far-field acoustic measurements. For the theoretical part, Tam and Tanna [14] and Tam [15] proposed a description of the noise-generation process based on the interaction between the instability waves and the shock-cell structure of the jet. Recently, new studies on the BBSAN have been performed, with the application of more recent diagnostic techniques [16] and more refined acoustic analyses [17].

While the BBSAN comes alongside screech in laboratory model jets, the latter does not seem to be observed in the practical full-scale problem. But screech is known to have a strong impact on the jet dynamics. It induces shock motion [18,19] and large-scale jet motion [20–22]. It also increases the spreading of the jet [23]. It is already known that screech has an effect on the BBSAN. Nagel et al. [24] and Norum [25] suppressed screech in a nonintrusive way and observed changes on the broadband hump, both in terms of frequency and amplitude (see, in particular, Fig. 10 of [25]). Tam [26] assumed that screech suppresses the BBSAN from comparisons between predicted and measured BBSAN spectra. He also suggested from the observation of the static pressure measurements by Norum and Seiner [12] that strong screech tones cause a rapid disintegration of the shock-cell structure, leading to the BBSAN attenuation. More recently, Morris and Miller [27] proposed two sets of calibration constants inside their numerical model for BBSAN prediction, designed specifically for the cases of screeching and non-screeching jets. The strong screech tones observed by the authors under flight conditions [22] also induced a strong attenuation of the BBSAN (see Fig. 17 in that paper). This is why much effort has long been devoted to screech suppression for BBSAN study. The nonintrusive suppression schemes quoted previously consist of a large baffle mounted upstream of the nozzle exit. However, this method is difficult to implement because the distance between the baffle and the nozzle exit has to be set for each screech frequency, hence for each operating condition. Rather than this technique, a small projection inside the nozzle lip, or tab, was extensively used. It clearly affects the shock-cell structure though. A loss of symmetry in the jet and a reduction of shock spacing were reported [11,24,28]. The effect on the measured shock noise also depends on the tab location with respect to the microphones. This

Received 30 April 2012; revision received 23 August 2012; accepted for publication 7 September 2012; published online 23 January 2013.

*Ph.D. Student, Université de Lyon, Laboratoire de Mécanique des Fluides et d'Acoustique, Unités Mixtes de Recherche–Centre National de la Recherche Scientifique 5509, 36 Avenue Guy de Collongue; benoit.andre@ec-lyon.fr (Corresponding Author).

†Université de Lyon, Laboratoire de Mécanique des Fluides et d'Acoustique, Unités Mixtes de Recherche–Centre National de la Recherche Scientifique 5509, 36 Avenue Guy de Collongue; Université Lyon 1, 43 Boulevard du 11 Novembre 1918, 69622 Villeurbanne Cedex; thomas.castelain@ec-lyon.fr.

‡Université de Lyon, Laboratoire de Mécanique des Fluides et d'Acoustique, Unités Mixtes de Recherche–Centre National de la Recherche Scientifique 5509, 36 Avenue Guy de Collongue; Institut Universitaire de France, 103 bd Saint-Michel, 75005 Paris; christophe.bailly@ec-lyon.fr.

arguably makes uncertain any conclusion on the BBSAN when screech is removed by such a device.

The use of long axial slots inside the nozzle wall as screech-suppressing device was initially proposed by Norum [29] and further investigated by Wlezien and Kibens [30] and Krothapalli et al. [31]. These studies report a strong screech attenuation, but their slots are bound to damage the BBSAN component as well due to their large depth. A nozzle with shallow notches cut into the lip was used at NASA (e.g., by Bridges and Wernet [32]) to study the BBSAN specifically. It has the advantage of reducing alterations to the jet structure. This strategy is tested in the present paper. Several experimental techniques are used to characterize the impact of the notches on the shock-cell structure and, finally, the effect of screech on the BBSAN. In the present study, a single shock-containing jet is investigated. It is, however, believed that this kind of simplified subscale model experiments can provide information of value to any research that performs a like study on a dual-flow nozzle jet corresponding to the full-scale problem.

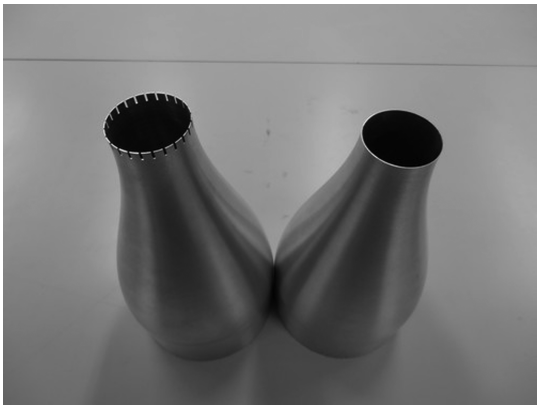

Fig. 1 Photograph of the notched nozzle (left) and the baseline nozzle (right).

II. Experimental Setup

A. Facility and Measurement Techniques

The supersonic jet is unheated and exhausts into an anechoic room. The experimental arrangement does not allow a total pressure probe to be introduced in the flow upstream of, and next to, the nozzle exit plane. Thus, the wall static pressure is measured approximately 15 nozzle diameters upstream of the exit. The stagnation pressure is then retrieved from the static pressure value through an estimate of the local Mach number in the measurement cross section. Finally, the stagnation pressure is used to evaluate the nozzle pressure ratio, defined as the ratio between stagnation and ambient pressure. In this paper, the operating condition will be expressed in terms of the ideally expanded jet Mach number M_j; the values of M_j investigated are 1.10, 1.15, 1.35, and 1.50. The stagnation temperature is measured by a thermocouple probe.

Far-field acoustic data are obtained from 13 6.35-mm-diam PCB Piezotronics condenser microphones fixed on a circular polar antenna 2020 mm from the center of the nozzle. They are set every 10 deg from 30 to 150 deg. In the following, polar angles are written θ and measured from the downstream jet axis. The transducers are used in normal incidence without protecting grid. Near-field acoustic data are also acquired using four 3.175-mm-diam G.R.A.S. Sound & Vibration transducers located at a distance of the order of one jet diameter from the lip line, depending on the operating condition of the jet. The microphones are set perpendicular to the jet axis and are mounted on an axial traverse. All microphone signals are sampled at 102,400 Hz by a National Instruments PXI 5733 board.

A Z-type schlieren system, mounted on an axial traverse downstream of the nozzle exit, has been used to visualize the flows exhausting through both nozzles. It consists of a light-emitting diode, two f/8, 203.2-mm-diam parabolic mirrors, a knife edge, and a high-speed numerical camera. The off-axis setting of the mirrors is limited to $2\alpha = 10$ deg. Refer to [33] for more details on the schlieren setup.

Static pressure measurements have been performed by means of short static probes of biconical shape, as designed by Pinckney [34]. The outer diameter of the probes is 1.5 mm, and the holes are located approximately 4.7 mm from the tip. Their compact geometry aims at solving the difficulty of measuring pressure in a flow with high gradients. Such probes have been extensively used for shock-cell structure characterizations, especially in connection with the BBSAN [12,35].

B. Screech-Reduction Method

Two different contoured convergent nozzles are used. One is a 38.25-mm-diam nozzle with smooth lips. The other, aimed at reducing screech tones, is a 38.7-mm-diam nozzle with 24 notches of 1 mm width (in the azimuthal direction) times 4 mm depth (in the jet direction). The size of the cuts has been determined from a small parametric study to obtain a good screech suppression. The notches are cut inside a 5-mm-long section of parallel walls terminating the nozzle. Both nozzles have a lip thickness of 0.5 mm. They are displayed in Fig. 1 and will be referred to as baseline and notched nozzle in the following.

Far-field acoustic spectra measured with both nozzles are presented in Fig. 2 for four values of M_j at $\theta = 110$ deg. They are plotted against the Strouhal number expressed as $Sr = fD_j/U_j$, with f as the frequency, D_j as the fully expanded jet diameter, and U_j as the perfectly expanded velocity. It is evident that the notches are very effective at $M_j = 1.15$, 1.35, and 1.50. However, the screech reduction is smaller at $M_j = 1.10$. The same conclusions can be reached when examining other polar angles.

III. Aerodynamical Effects of the Screech-Suppressing Method

The influence of the nozzle indentation on the jet development, especially on the shock-cell structure, is now considered. It was recalled in the Introduction that intrusive screech-suppressing methods, such as tabs, deeply alter the shock structure. It is essential that the effect of the canceling technique on the jet be as small as possible to be able to relate unambiguously any change in the BBSAN shape to the screech reduction only.

Because screech has an effect on the jet dynamics, the notched nozzle will indirectly induce modifications in the jet development through the screech suppression. A separation of the effects of the notches and screech is performed here, based essentially on the recognition that screech modifies the *downstream* shock-cell structure. In this section, the experimental results are presented first without analysis. Then, the direct effect of the notches is addressed, followed by the effect of screech. Finally, the reason why the notches are efficient at suppressing screech is discussed.

A. Experimental Results

Mean schlieren pictures obtained by averaging of 500 instantaneous images sampled at 500 Hz are shown in Figs. 3 and 4 for $M_j = 1.10$ and 1.35, respectively. Each picture results from a collage of four partial mean images taken at different axial stations along the jet. Because of its indentation, it is not clear where the shock-cell structure actually starts in the case of the notched nozzle. To circumvent this issue, the first shocks of both jets are axially aligned for each M_j. The subsequent shock-cell development can then be directly compared.

Measurements of static pressure P_s have been performed on the jet centerline at $M_j = 1.10$ and 1.35 with both nozzles. The results are presented in Fig. 5, in which the P_s profiles for the notched nozzle have been translated downstream for the first shocks to be approximately aligned with their baseline counterparts. Some comments on the intrusive character of the measurements are first required. The presence of the probe and its support inside the jet modifies screech. When the probe is in the first few shock cells, no screech tone is emitted by either nozzle. From this region, the direct effect of the notches can be assessed (see Sec. III.B). When the probe

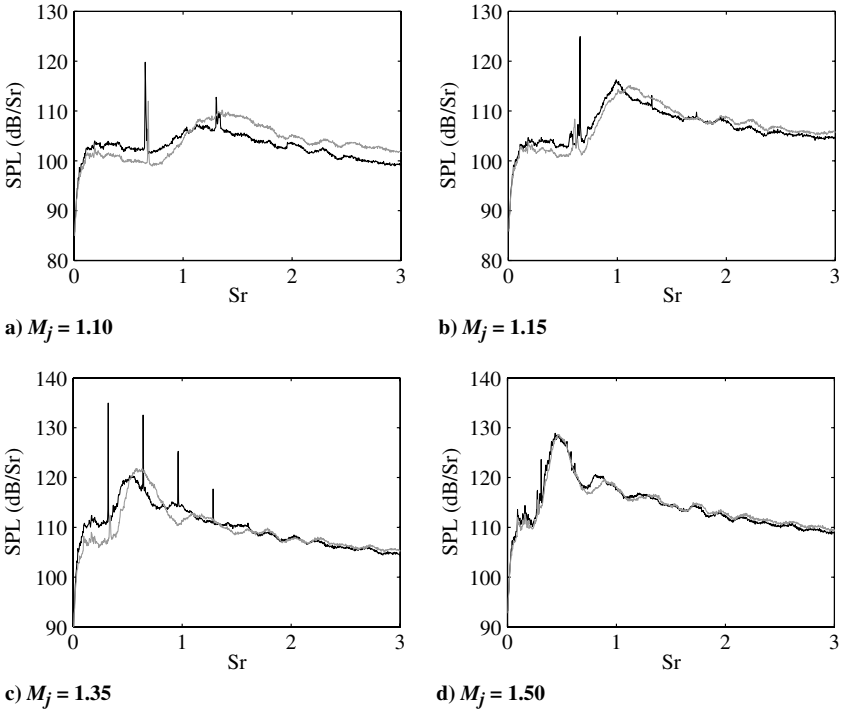

Fig. 2 Far-field acoustic spectra measured at a polar angle $\theta = 110$ deg (from the downstream direction). $Sr = fD_j/U_j$. Baseline nozzle (dark line) and notched nozzle (grey line). SPL denotes sound pressure level.

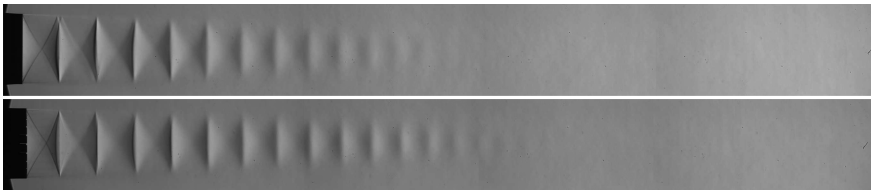

Fig. 3 Schlieren visualizations with the baseline (top) and notched (bottom) nozzle, $M_j = 1.10$.

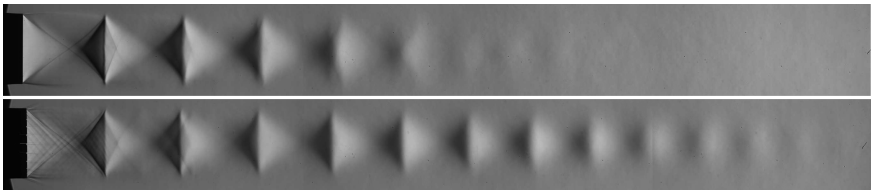

Fig. 4 Schlieren visualizations with the baseline (top) and notched (bottom) nozzle, $M_j = 1.35$.

is further downstream, a tone is detected, whose level and frequency depend on the location of the probe, although it was checked that the screech frequency of the free jet prevails. For $M_j = 1.10$, the emergence of this tone above the background level was seen to be much smaller for the notched nozzle. For $M_j = 1.35$, no tone was recorded with the notched nozzle, whereas the baseline case sustained very strong screech tones as of the position marked by a dashed line in Fig. 5b. As a consequence, the effect of screech can be

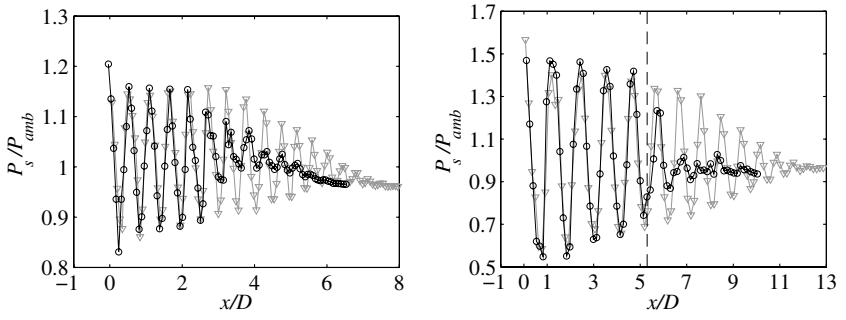

Fig. 5 Centerline static pressure profiles. Baseline nozzle (○) and notched nozzle (▽). P_{amb} is the ambient pressure, x is the axial coordinate, and D is the nozzle diameter. The dashed line in b) marks the probe location for which strong screech tones first appeared during the baseline traverse.

inferred from the downstream part of the shock-cell structure (see Sec. III.C).

B. Direct Effect of the Notches

On the schlieren pictures in Figs. 3 and 4, the direct effect of the notches can be deduced from the comparison of the first shock cells. The jet development is not strongly affected by the change in the nozzle-lip geometry: the shock system remains axisymmetric in the case of the notched nozzle, and the shock spacing between the baseline and the notched case is unchanged at $M_j = 1.10$. The latter statement is only approximate at $M_j = 1.35$. Indeed, the second shock cell is shorter with the notched nozzle, but the shock spacing remains approximately unchanged afterward. Concerning the first cell, the effect of the indentation is clearer at $M_j = 1.35$ than at $M_j = 1.10$. This comes from the larger degree of underexpansion at the higher M_j. The greater pressure ratio across the slots between jet and ambient induces an ejection through them, especially visible on those located in the vertical plane, as well as a more complex pattern in the first shock cell.

The limited effect of the notches on the shock-cell structure is quantitatively confirmed by the static pressure profiles in the first shock cells, where screech is suppressed for both nozzles by the probe intrusion. The shock-cell strength, which can be deduced from the amplitude of oscillation of the static pressure, is indeed very similar in this region for both nozzles.

By examining the instantaneous schlieren images, the mixing layers are found to be thickened by the slots. However, upon inspection of the narrowband acoustic spectra for the sonic jet ($M_j = 1.0$) for both $\theta = 30$ and 110 deg, little effect is observed on the turbulent mixing noise when no shock-cell structure exists. The spectra are displayed in Fig. 6. It is thus expected that the small-scale and large-scale turbulence, responsible for the turbulent mixing noise [36,37], are preserved by the notches.

Finally, the closeness of the broadband humps of the BBSAN in the acoustic spectra of Fig. 2d, at a condition where none of the two nozzles emitted strong screech tones, shows the very limited effect of the notches on the BBSAN component.

C. Effect of Screech on the Jet Development

Going back to the schlieren images in Figs. 3 and 4, it seems that the shock system extends further downstream for the notched nozzle at $M_j = 1.10$, with more shocks being visible. This conclusion is also true, albeit much clearer, at $M_j = 1.35$. The difference between $M_j = 1.10$ and 1.35 may be linked with the screech-suppressing efficiency of the notched nozzle (see Fig. 2). A strong screech tone, showing several harmonics, is completely suppressed by the indentation at $M_j = 1.35$, whereas it was noticed that the notched nozzle was less effective at $M_j = 1.10$. Hence, eliminating screech more thoroughly entails a greater extension of the shock system. It can then be inferred that screech is responsible for a quicker damping of the time-averaged shock-cell structure.

It was said previously that strong screech tones were emitted during the static pressure measurements at $M_j = 1.35$ with the baseline nozzle, downstream of the location marked by a dashed line in Fig. 5b. Meanwhile, no screech tones were radiated by the notched nozzle. The appearance of strong screech tones is thus correlated with the observed breakdown of the shock-cell structure. Hence, it can also be concluded from the pressure measurements that screech is responsible for a quicker damping of the time-averaged shock-cell structure.

This conclusion is corroborated by other investigations. Glass [23] presented shadowgrams, which show this effect of screech. The shock-cell structure of the rectangular jet investigated by Norum [38] also extended much further downstream as soon as screech ceased to exist. The cessation occurred at high M_j, in agreement with Raman [39], whose static pressure profiles also support this observation. Norum [38] proposed the alleviation of the jet oscillation as a cause for the extension of the shock-cell pattern (see also Fig. 3 in Raman et al. [40]). In the present study, some high-speed schlieren recordings of the pressure probe inside the jet at $M_j = 1.35$ also strongly suggest that the screech-induced jet oscillation may be responsible for the quicker damping of the shock-cell structure. The mechanism leading to the damping probably involves the enhanced mixing induced by screech [23].

D. How Notches Suppress Screech

The reason why the notched nozzle is efficient at suppressing screech is now briefly discussed. It can be gathered from the schlieren visualizations that the jet flow near the nozzle lips is quite different between the two nozzles. The response of a jet near the nozzle exit to upstream propagating screech waves, also termed receptivity, is a part of the feedback loop explaining screech. Raman et al. [40] studied this part of the loop and concluded to a continuous coupling of acoustic waves and shear layer, but on a short distance after the nozzle exit. The slots probably disrupt the receptivity of the shear layer in modifying its very beginning. From this assumption, the smaller influence of the indentation noticed at $M_j = 1.10$ on the initial shear layer may explain the weaker screech-suppressing efficiency, as compared to higher degrees of underexpansion. Moreover, the explanation of the phenomenon of screech cessation at high M_j proposed by Raman [39] may just as well apply here: the ejection through the notches visible on the schlieren pictures could block the upstream propagating acoustic waves, thus preventing the closing of the feedback loop. This remains to be verified in future work.

IV. Screech Effects on the Broadband Shock-Associated Noise Component

It has been shown in the previous section that the notches in themselves had a small effect on the jet development. It is thus postulated in the following that the differences between the BBSAN from the two nozzles can be entirely attributed to the different screech-tone levels. Some salient features are already visible in Fig. 2: the broadband hump is usually enhanced and shifted to higher frequencies. The modifications of the BBSAN are examined more thoroughly here, from far-field and near-field acoustic measurements.

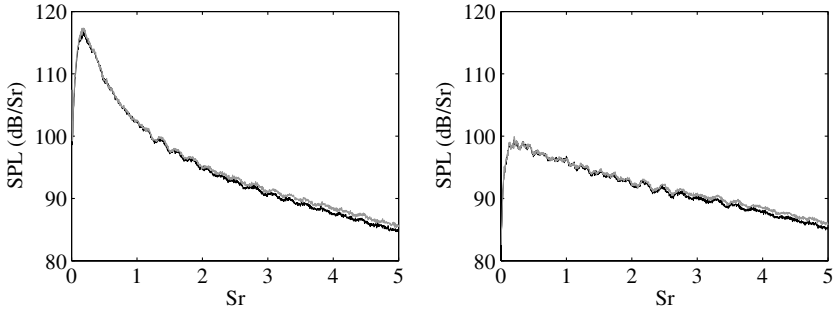

a) $\theta = 30$ deg b) $\theta = 110$ deg

Fig. 6 Far-field acoustic spectra, $M_j = 1.0$. Baseline nozzle (dark line) and notched nozzle (grey line). SPL denotes sound pressure level.

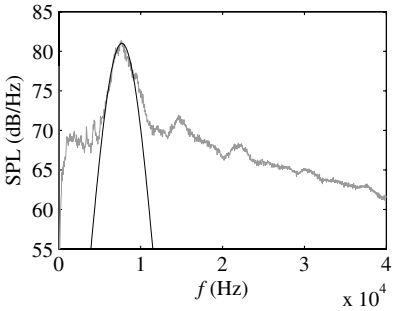

Fig. 7 Analysis of the first broadband hump. Far-field acoustic spectrum measured at $\theta = 90$ deg, $M_j = 1.35$ with the notched nozzle (grey line), and Gaussian fit (dark line). SPL denotes sound pressure level.

A. Far-Field Acoustic Measurements

To quantitatively analyze the first broadband hump of the acoustic spectra in a systematical way, a Gaussian curve writing

$$A \exp[-(f - f_p)^2/(2\sigma^2)] \tag{1}$$

is fitted to each spectrum. In Eq. (1), A is the maximum amplitude of the hump, f is the frequency, f_p is the peak frequency, and σ is a measure of the hump width. An example of fitting is shown in Fig. 7.

A detailed traverse of the M_j range from 1.0 to 1.55 has been performed for each nozzle, and far-field acoustic spectra have been measured at each operating point. For every value of M_j, the first broadband hump in the spectrum measured at $\theta = 90$ deg has been fitted by a Gaussian curve, and the Strouhal number based on the peak frequency, Sr_p, has been plotted in Fig. 8. Obviously, the peak Strouhal number is decreasing with an increasing M_j, owing to the lengthening of the shock cells. In most cases, Sr_p is larger for the notched nozzle than for the baseline. This property is in agreement with the baffle experiments of Norum [25]. But the most interesting feature is the tuning existing between Sr_p and two times Sr_s for the baseline nozzle (Sr_s is the screech Strouhal number). The Sr_p curve clearly follows the staging process of screech in the baseline configuration, whereas for the notched nozzle, Sr_p evolves smoothly through the M_j range. (The jump above $M_j = 1.20$ for the notched nozzle is due to a change of interpretation of a continuously evolving hump.) This tuning can be related to modifications in the shock spacing or the convection velocity due to the screech staging, which should not occur in the absence of screech. Moreover, inside ranges where two screech frequencies exist in the baseline case, like around $M_j = 1.25$ and 1.40, the broadband hump seems to settle in-between the two tones. The existence of an effect of screech on the BBSAN is clearly demonstrated by Fig. 8.

The evolution of the BBSAN peak frequency has been estimated over all directivity angles of the far-field antenna for several values of M_j. The nondimensioned peak wavelength λ_p/D is plotted against $\cos\theta$ in Fig. 9. First, it is clear that λ_p is smaller in the case of the notched nozzle, over the entire θ and M_j range, leading to a higher peak frequency of the BBSAN when screech is suppressed, as was visible in Fig. 2. It is worth noting that the nondimensioned peak wavelengths are very close at $M_j = 1.50$, where the baseline screech tones were weak and unsettled between two modes (see Figs. 2d and 8).

Second, all the curves are approximately linear. This comes from the well-known Doppler effect arising on the far-field peak frequencies of the BBSAN. Harper-Bourne and Fisher [9] and Tam and Tanna [14] derived the following expression for f_p:

$$f_p = \frac{U_c}{L(1 - M_c \cos\theta)} \tag{2}$$

from two distinct theoretical approaches. In Eq. (2), U_c is the convection velocity of the vortical structures responsible for shock noise, M_c is U_c divided by the ambient speed of sound, and L is the shock spacing. Seiner and Yu [41] used this relation to estimate the convection velocity, by noting that

$$\lambda_p(\theta)/\lambda_p(\theta = 90 \text{ deg}) = 1 - M_c \cos\theta$$

The same procedure has been applied here for the two nozzles. The resulting values of U_c/U_j are displayed in Table 1. There is a striking difference between the baseline and the notched nozzle. While the U_c/U_j estimate for the latter is constant with M_j, the estimate for the former keeps rising. At $M_j = 1.50$, both estimates are equal, owing to the weak baseline screech as mentioned previously. The estimate at $M_j = 1.10$ for the baseline nozzle appears to be very low as compared with usual values from the literature, which could partly arise from the limited number of data points available and the shallowness of the broadband hump over the turbulent mixing noise, making detection more subjective and peak frequencies more uncertain. Panda et al. [42] also found screech mode dependence for convection velocity. When screech is removed, so is the variation of U_c/U_j as well, and the classical value $U_c/U_j \approx 2/3$ is then obtained.

B. Near-Field Acoustic Measurements

The cases $M_j = 1.10$ and $M_j = 1.35$ have also been studied in the acoustic near field. Results for only $M_j = 1.10$ are reported here, because similar conclusions are reached at the higher Mach number. The 3.175-mm-diam transducers are located 4.9 mm away from the lip line and are moved along the jet. Sample spectra for both nozzles are presented in Fig. 10. The baseline broadband hump is not as pronounced as that of the notched nozzle. The maximum amplitude of the hump has simply been read for each near-field spectrum, and its evolution along the jet plume is shown in Fig. 11. Similar to the results of Seiner and Yu [13], the downstream shock cells are seen to be stronger BBSAN sources than the first ones. Apart from a limited region around $x/D = 4$, where the entire spectra for the notched nozzle inexplicably dropped, the broadband hump with this nozzle clearly dominates that of the baseline nozzle. Moreover, this tendency is emphasized for the downstream shock cells. This may be linked to the schlieren visualizations and pressure measurements

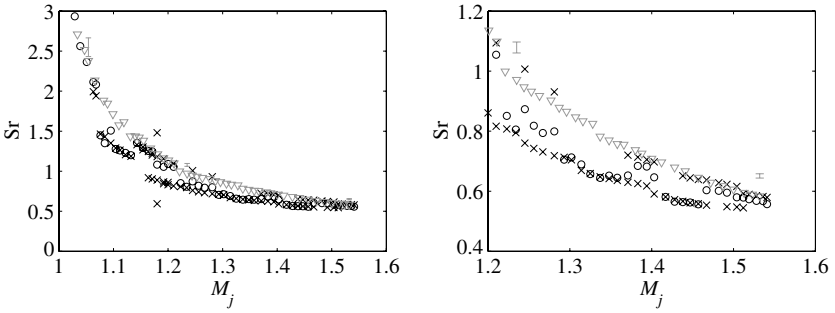

Fig. 8 a) Evolution of the screech and BBSAN Strouhal number against M_j. b) Enlargement of (a) in the upper M_j region. Sr_p for the baseline nozzle (○), Sr_p for the notched nozzle (▽), and two times Sr_s (baseline nozzle, ×). The bars over $M_j = 1.05$, 1.24 and 1.53 denote uncertainty ranges (notched nozzle).

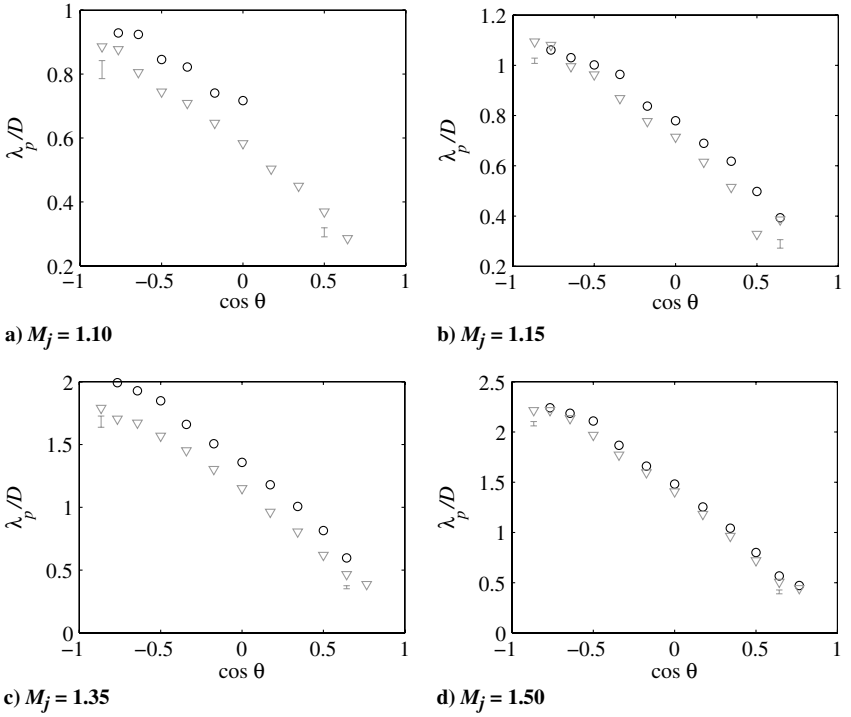

Fig. 9 Evolution of the nondimensioned peak wavelength λ_p/D against cos θ. Baseline nozzle (○) and notched nozzle (∇). The bars denote the uncertainty ranges as estimated for the notched nozzle.

shown in Sec. III. A strong screech was said to accelerate the damping of the shock-cell structure, so that fewer cells were visible with the baseline nozzle. As a result, the downstream shock cells are responsible for higher levels of BBSAN in the event of a weak screech than with strong screech tones.

The estimation of the peak frequencies of the near-field broadband humps is presented in Fig. 12. A progressive shift to higher frequencies is apparent as the microphones are moved downstream. This phenomenon is in agreement with similar measurements performed by Norum and Seiner [11]. It seems that the downstream part of the shock-cell system emits a shock-associated noise of higher frequency. This shift of near-field f_p with downstream distance could be the reason for the observed difference in far-field peak frequencies between the two nozzles. When screech is stronger, the downstream shock cells are weakened so that the contribution of these cells to the overall BBSAN levels is smaller, resulting in a reduced peak frequency of emission.

C. Effect of Screech on the Amplitude of the Broadband Shock-Associated Noise

The effect of screech on the BBSAN amplitude in the far field is discussed now. The methodology developed by Viswanathan [43] and Viswanathan et al. [17] is used here, in which turbulent mixing noise is assumed not to be modified by shocks. Furthermore, a universal shape for the turbulent mixing noise is assumed for each directivity angle and stagnation temperature. The master shape is obtained by plotting

$$\mathrm{SPL} - 10\log_{10}(A_j/A_{\mathrm{ref}}) - 10n\log_{10}(U_j/c_\infty) - 10\log_{10}(D_j/U_j) \tag{3}$$

Table 1 Values of U_c/U_j found from a linear curve fitting of $\lambda_p(\theta)/\lambda_p(\theta = 90\ \mathrm{deg})$

		M_j			
		1.10	1.15	1.35	1.50
U_c/U_j	Baseline	0.42	0.58	0.61	0.65
	Notched	0.66	0.65	0.65	0.65

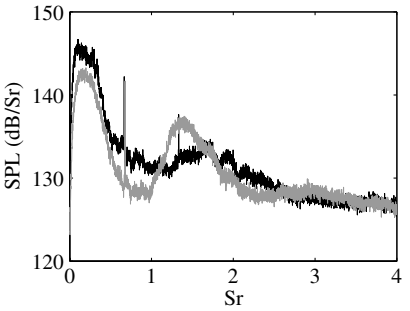

Fig. 10 Near-field acoustic spectra, acquired at $M_j = 1.10$, $x/D = 5.8$, $y = D/2 + 4.9$ mm. Baseline nozzle (dark line) and notched nozzle (grey line). SPL denotes sound pressure level.

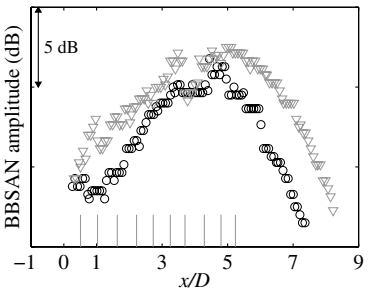

Fig. 11 Peak amplitude of the broadband hump in the near field, $M_j = 1.10$. Baseline nozzle (○) and notched nozzle (∇). The vertical lines denote the locations of the first 10 shocks (notched nozzle).

against the Strouhal number. In Eq. (3), A_j is the flow fully expanded area, A_{ref} is a reference area taken as 1 m^2, n is a velocity exponent depending on θ and the total temperature (see [43]), and c_∞ is the ambient speed of sound. A_j has to be computed from the perfectly expanded jet diameter D_j, which depends on M_j.

In the present case, the master shapes for each angle have been estimated for the two nozzles by considering the spectra of the sonic jet ($M_j = 1.0$). Then, the mixing noise component has been

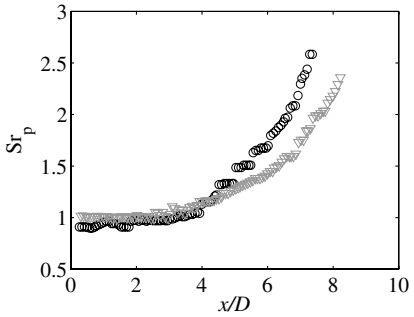

Fig. 12 Peak Strouhal number of broadband shock noise in the near field, $M_j = 1.10$. Baseline nozzle (○) and notched nozzle (∇).

subtracted from the total far-field spectra, and the total shock-noise levels have been obtained by integration over the Strouhal-number range. When present, screech has been numerically removed from the far-field spectra to obtain an estimation of the BBSAN levels alone.

The results for $M_j = 1.10$, 1.15, 1.35, and 1.50 are presented in Fig. 13. The directivity of the BBSAN is first discussed. The BBSAN for the two higher Mach numbers seems to be roughly omnidirectional. This property has already been noted in the literature (see, e.g., Tanna [10] and Viswanathan et al. [17]). An undulation in the levels is visible however, which is similar for both values of M_j and can also be observed in the measurements of Viswanathan et al. for a cold jet at $M_j = 1.36$ (see their Fig. 15). No explanation is proposed to interpret this result. At $M_j = 1.10$ and 1.15, a clear tendency for the BBSAN levels to increase in the upstream direction is identified, and the omnidirectionality is reached for $\theta \geq 100$ deg. Now, the comparison of the sound pressure levels between the two nozzles is mentioned. The closeness of the levels at $M_j = 1.50$ for the two nozzles is in agreement with the spectra shown in Fig. 2, and confirms that the notches have a limited effect on the BBSAN emission, the screech being similar in both configurations. At the other values of M_j, the BBSAN levels are higher when screech is absent, which was already suggested by several reseachers, as mentioned in the Introduction. However, this feature is less pronounced for $M_j = 1.35$ than for $M_j = 1.10$, although the former operating condition presented the higher screech tones. Overall, it seems that screech reduces the BBSAN levels to an extent depending on the operating condition and the polar angle.

V. Conclusions

The effect of screech tones on the broadband shock-associated noise (BBSAN) has been studied experimentally. The screech-suppression technique consists in indentations in the nozzle lip. This strategy proved effective for all fully expanded Mach numbers investigated. It has been checked on schlieren visualizations and static pressure measurements that this technique did not disrupt the shock-cell structure, which is not the case when an intrusive tab is used. Especially, the shock spacing is almost unchanged when using the notched nozzle. An extension of the shock-cell pattern with the notched nozzle has been identified, which leads to the conclusion that strong screech tones accelerate the damping of the shock-cell structure.

Far-field acoustic measurements have shown that screech has an important effect on the BBSAN. The existence of a tuning between the BBSAN peak frequency f_p and the screech frequency has been made clear from the evolution of these frequencies with M_j. The screech modal behavior produces screech-frequency discontinuities in this evolution, which are also visible on f_p. They disappear when the screech is removed. This tuning is an indication that the screech's staging process has enough influence on the jet dynamics to affect the BBSAN. The variations of f_p with directivity angle have been estimated, which has led to an assessment of the convection velocity for several Mach numbers. It has been shown that the ratio of convection velocity over jet velocity was independent on M_j, at least in the range tested, when the screech was eliminated. This is in contrast with the mode-related variation of U_c/U_j in screeching jets. The increase of f_p when the screech is suppressed has been confirmed. Near-field acoustic measurements have offered an explanation for this property. Indeed, an f_p shift to higher frequencies when the near-field microphones move downstream has been identified for the baseline and notched nozzles, along with an extension of the source region for the BBSAN when screech is absent. The assumption here is that an excess in high-frequency content is produced by the additional shock cells existing far

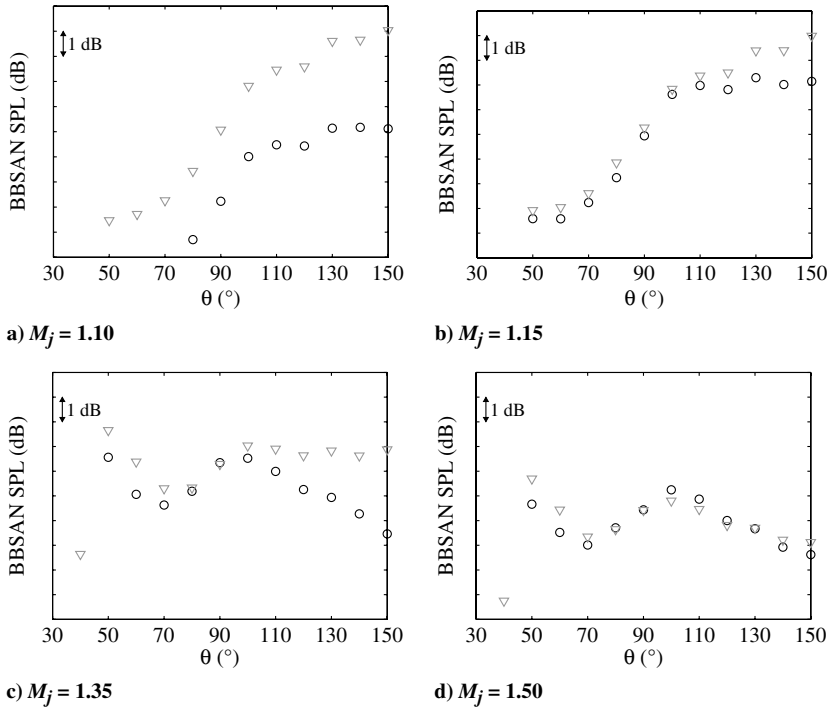

Fig. 13 Total sound pressure level (SPL) associated to the BBSAN, computed from the far-field acoustic spectra. Baseline nozzle (○) and notched nozzle (∇).

downstream when screech is suppressed. Finally, the total far-field levels of broadband shock noise have been extracted from the complete spectra. They have been shown to increase when screech was eliminated. This trend was observed consistently for the various values of M_j and θ considered.

More detailed aerodynamical measurements are needed to identify the modifications of the turbulence with and without screech, which has obviously a direct bearing on the BBSAN. Especially, the relation between the BBSAN generation and the motion of the vortical structures with respect to the shocks could be investigated. Indeed, screech has a possible effect on the BBSAN simply because of the fact that the shocks oscillate at the screech frequency in a screeching jet.

Acknowledgments

The authors wish to thank Airbus Operations S.A.S. (Mauro Porta) and Snecma (Guillaume Bodard) for their joint financial support.

References

[1] Powell, A., "On the Mechanism of Choked Jet Noise," *Proceedings of the Physical Society of London*, Vol. 66, No. 408, 1953, pp. 1039–1056. doi:10.1088/0370-1301/66/12/306

[2] Merle, M., Sur la Fréquence des Ondes émises par un Jet d'air à Grande Vitesse, *Compte Rendu de l'Académie des Sciences (France)*, Vol. 243, 1956, pp. 490–493.

[3] Davies, M. G., and Oldfield, D. E. S., "Tones from a Choked Axisymmetric Jet I. Cell Structure, Eddy Velocity and Source Locations," *Acustica*, Vol. 12, No. 4, 1962, pp. 257–267.

[4] Davies, M. G., and Oldfield, D. E. S., "Tones from a Choked Axisymmetric Jet II. The Self Excited Loop and Mode of Oscillation," *Acustica*, Vol. 12, No. 4, 1962, pp. 267–277.

[5] Powell, A., Umeda, Y., and Ishii, R., "Observations of the Oscillation Modes of Choked Circular Jets," *Journal of the Acoustical Society of America*, Vol. 92, No. 5, 1992, pp. 2823–2836. doi:10.1121/1.404398

[6] Raman, G., "Supersonic Jet Screech: Half-Century from Powell to the Present," *Journal of Sound and Vibration*, Vol. 225, No. 3, 1999, pp. 543–571. doi:10.1006/jsvi.1999.2181

[7] Tam, C. K. W., Seiner, J. M., and Yu, J. C., "Proposed Relationship Between Broadband Shock Associated Noise and Screech Tones," *Journal of Sound and Vibration*, Vol. 110, No. 2, 1986, pp. 309–321. doi:10.1016/S0022-460X(86)80212-7

[8] Martlew, D. L., *Noise Associated with Shock Waves in Supersonic Jets*, AGARD CP 42, 1969, pp. 7-1–7-10.

[9] Harper-Bourne, M., and Fisher, M. J., *The Noise from Shock Waves in Supersonic Jets*, AGARD CP 131, 1973, pp. 11-1–11-13.

[10] Tanna, H. K., "An Experimental Study of Jet Noise Part II: Shock Associated Noise," *Journal of Sound and Vibration*, Vol. 50, No. 3, 1977, pp. 429–444. doi:10.1016/0022-460X(77)90494-1

[11] Norum, T. D., and Seiner, J. M., "Broadband Shock Noise from Supersonic Jets," *AIAA Journal*, Vol. 20, No. 1, 1982, pp. 68–73. doi:10.2514/3.51048

[12] Norum, T. D., and Seiner, J. M., "Measurements of Mean Static Pressure and Far Field Acoustics of Shock Containing Supersonic Jets," NASA TM 84521, 1982.

[13] Seiner, J. M., and Yu, J. C., "Acoustic Near-Field Properties Associated with Broadband Shock Noise," *AIAA Journal*, Vol. 22, No. 9, 1984, pp. 1207–1215. doi:10.2514/3.8762

[14] Tam, C. K. W., and Tanna, H. K., "Shock Associated Noise of Supersonic Jets from Convergent–Divergent Nozzles," *Journal of Sound and Vibration*, Vol. 81, No. 3, 1982, pp. 337–358. doi:10.1016/0022-460X(82)90244-9

[15] Tam, C. K. W., "Jet Noise Generated by Large-Scale Coherent Motion," *Aeroacoustics of Flight Vehicles: Theory and Practice*, edited by Hubbard, H. H., Vol. 1, Noise Sources, NASA Langley Research Center, Hampton, VA, 1991, pp. 311–390.

[16] Veltin, J., Day, B. J., and McLaughlin, D. K., "Correlation of Flowfield and Acoustic Field Measurements in High-Speed Jets," *AIAA Journal*, Vol. 49, No. 1, 2011, pp. 150–163. doi:10.2514/1.J050583

[17] Viswanathan, K., Alkislar, M. B., and Czech, M. J., "Characteristics of the Shock Noise Component of Jet Noise," *AIAA Journal*, Vol. 48, No. 1, 2010, pp. 25–46. doi:10.2514/1.38521

[18] Panda, J., "Shock Oscillation in Underexpanded Screeching Jets," *Journal of Fluid Mechanics*, Vol. 363, May 1998, pp. 173–198. doi:10.1017/S0022112098008842

[19] André, B., Castelain, T., and Bailly, C., "Shock Oscillations in a Supersonic Jet Exhibiting Antisymmetrical Screech," *AIAA Journal*, Vol. 50, No. 9, 2012, pp. 2017–2020. doi:10.2514/1.J051802

[20] Hammitt, A. G., "The Oscillation and Noise of an Overpressure Sonic Jet," *Journal of the Aerospace Sciences*, Vol. 28, No. 9, 1961, pp. 673–680.

[21] Sherman, P. M., Glass, D. R., and Duleep, K. G., "Jet Flow Field During Screech," *Applied Scientific Research*, Vol. 32, No. 3, 1976, pp. 283–303. doi:10.1007/BF00411780

[22] André, B., Castelain, T., and Bailly, C., "Experimental Study of Flight Effects on Screech in Underexpanded Jets," *Physics of Fluids*, Vol. 23, No. 12, 2011, pp. 1–14. doi:10.1063/1.3671735

[23] Glass, D. R., "Effects of Acoustic Feedback on the Spread and Decay of Supersonic Jets," *AIAA Journal*, Vol. 6, No. 10, 1968, pp. 1890–1897. doi:10.2514/3.4897

[24] Nagel, R. T., Denham, J. W., and Papathanasiou, A. G., "Supersonic Jet Screech Tone Cancellation," *AIAA Journal*, Vol. 21, No. 11, 1983, pp. 1541–1545. doi:10.2514/3.60153

[25] Norum, T. D., "Control of Jet Shock Associated Noise by a Reflector," AIAA Paper 84-2279, Oct. 1984.

[26] Tam, C. K. W., "Broadband Shock-Associated Noise of Moderately Imperfectly Expanded Supersonic Jets," *Journal of Sound and Vibration*, Vol. 140, No. 1, 1990, pp. 55–71. doi:10.1016/0022-460X(90)90906-G

[27] Morris, P. J., and Miller, S. A. E., "Prediction of Broadband Shock-Associated Noise Using Reynolds-Averaged Navier–Stokes Computational Fluid Dynamics," *AIAA Journal*, Vol. 48, No. 12, 2010, pp. 2931–2943. doi:10.2514/1.J050560

[28] Bryce, W. D., and Pinker, R. A., "The Noise from Unheated Supersonic Jets in Simulated Flight," AIAA Paper 77-1327, Oct. 1977.

[29] Norum, T. D., "Screech Suppression in Supersonic Jets," *AIAA Journal*, Vol. 21, No. 2, 1983, pp. 235–240. doi:10.2514/3.8059

[30] Wlezien, R. W., and Kibens, V., "Influence of Nozzle Asymmetry on Supersonic Jets," *AIAA Journal*, Vol. 26, No. 1, 1988, pp. 27–33. doi:10.2514/3.9846

[31] Krothapalli, A., McDaniel, J., and Baganoff, D., "Effect of Slotting on the Noise of an Axisymmetric Supersonic Jet," *AIAA Journal*, Vol. 28, No. 12, 1990, pp. 2136–2138. doi:10.2514/3.10534

[32] Bridges, J. E., and Wernet, M. P., "Turbulence Associated with Broadband Shock Noise in Hot Jets," NASA TM 215274, 2008.

[33] Settles, G. S., *Schlieren and Shadowgraph Techniques*, Springer, Berlin/Heidelberg, 2001, pp. 42–46.

[34] Pinckney, S. Z., "A Short Static-Pressure Probe Design for Supersonic Flow," NASA TN D-7978, 1975.

[35] Norum, T. D., and Shearin, J. G., "Shock Structure and Noise of Supersonic Jets in Simulated Flight to Mach 0.4," NASA TP 2785, 1988.

[36] Bogey, C., and Bailly, C., "An Analysis of the Correlations Between the Turbulent Flow and the Sound Pressure Fields of Subsonic Jets," *Journal of Fluid Mechanics*, Vol. 583, July 2007, pp. 71–97. doi:10.1017/S002211200700612X

[37] Tam, C. K. W., Viswanathan, K., Ahuja, K. K., and Panda, J., "The Sources of Jet Noise: Experimental Evidence," *Journal of Fluid Mechanics*, Vol. 615, Nov. 2008, pp. 253–292. doi:10.1017/S0022112008003704

[38] Norum, T. D., "Supersonic Rectangular Jet Impingement Noise Experiments," *AIAA Journal*, Vol. 29, No. 7, 1991, pp. 1051–1057. doi:10.2514/3.10703

[39] Raman, G., "Cessation of Screech in Underexpanded Jets," *Journal of Fluid Mechanics*, Vol. 336, April 1997, pp. 69–90. doi:10.1017/S002211209600451X

[40] Raman, G., Panda, J., and Zaman, K. B. M. Q., "Feedback and Receptivity During Jet Screech: Influence of an Upstream Reflector," AIAA Paper 97-0144, Jan. 1997.
[41] Seiner, J. M., and Yu, J. C., "Acoustic Near Field and Local Flow Properties Associated with Broadband Shock Noise," AIAA Paper 81-1975, Oct. 1981.
[42] Panda, J., Raman, G., and Zaman, K. B. M. Q., "Underexpanded Screeching Jets from Circular, Rectangular and Elliptic Nozzles," AIAA Paper 97-1623, 1997.
[43] Viswanathan, K., "Scaling Laws and a Method for Identifying Components of Jet Noise," *AIAA Journal*, Vol. 44, No. 10, 2006, pp. 2274–2285.
doi:10.2514/1.18486

A. Lyrintzis
Associate Editor